Silicon Nitride Spot Size Converter With Very Low-Loss Over the C-Band

G. Brunetti, R. Heuvink, E. Schreuder, M. N. Armenise, and C. Ciminelli, *Senior Member, IEEE*

***Abstract*— Photonic Integrated Circuits (PIC) provide a solution to overcome the main limitations of electronics, such as the operating frequency and heat generation, pushing the so-called "More than Moore" concept to increase the capacity and the speed of data transmission. In large data centers and optical transmission systems, PICs are interconnected by using fiber-to-chip couplers, which are crucial to improve system performance. An ultra-low loss interconnection (<1 dB) over a wide bandwidth (≈50 nm) is the gold standard. In this context, the silicon nitride (Si_3N_4) platform is a promising candidate, with propagation losses of the order of dB/m at 1550 nm. Here, we propose the design and the experimental results for a silicon nitride-based fiber-to-chip interconnect, acting as a high aspect ratio waveguide Spot-Size Converter (SSC). A coupling loss less than 0.20 dB over the entire C-band and within a footprint of 1,800 μm^2 has been experimentally demonstrated, suggesting the proposed interconnect as a promising solution for next-generation high-density PICs.**

***Index Terms*— Interconnections, photonic integrated circuits, silicon photonics, spot size converter.**

I. Introduction

COMPLEX optical transmission systems present a large number of optical interconnects between fibers and Photonic Integrated Circuits (PICs) [1], [2]. High-efficiency data transmission requires an effective fiber-to-chip coupling to reduce the system insertion loss [3]. In particular, the major sources of losses in PICs are coupling and scattering ones. In recent years, significant research effort has been spent both to reduce scattering losses by engineering waveguides with a small overlap of the field with rough sidewalls [4], and to investigate new optical materials, such as silicon nitride (Si_3N_4) [5], also improving the manufacturing processes. Based on the approach above, scattering losses < 1 dB/m at 1550 nm have been achieved by using high-aspect ratio Si_3N_4 waveguide, paving the way for their use in applications where losses are a crucial concern [6]. Coupling losses still remain the major issue, which requires non-trivial engineering of the fiber-to-chip interconnects.

Butt coupling between a single-mode Si-based or SiN waveguide and a Single Mode Fiber (SMF) leads to large coupling losses (> 20 dB). According to the optical modes overlapping theory [7], these are caused by the large mismatch between the Mode Field Diameter (MFD) of the SMF (≈ 10 μm) [8] and the waveguide core (which is on the order of hundreds of nm). Such a mismatch is not suitable for PIC systems [9]. To overcome this limitation, two coupling techniques have been proposed in the literature, including the butt-coupling, also called edge coupling or in-plane coupling [10], [11], [12], [13], [14], [15], [16], [17], and the grating coupler, also called vertical coupling or off-plane coupling [18], [19], [20], [21], [22], [23]. Both aim at improving the performance in terms of coupling efficiency, bandwidth, polarization sensitivity and CMOS compatibility.

For the grating coupler, the fiber is placed above the device vertically or at a tiny angle to improve efficiency. Grating couplers show several advantages, including compact size, flexible coupling position, and wafer-level testing capability. However, they suffer from large coupling losses (>1 dB for TE and >3 dB for TM), narrow bandwidth (<80 nm @ 3dB) [19], [20], [21], [22], [23] and an off-plane nature that makes their integration into PICs for next-generation networks difficult. The large coupling losses are mainly caused by the Fresnel reflections at the air/silicon interface [18].

For the butt-coupling regime, the fiber is placed close to the wafer facets and horizontally aligned with the waveguide. The inverse taper coupler is the straightforward edge coupler that acts as a Spot Size Converter (SSC), which is able to adiabatically expand both the silicon waveguide mode and the effective refractive index for an appropriate fiber matching, thus reducing the related mismatch. At the input stage, the fiber mode surrounds the SSC tip up to a certain length where the mode is compressed into a guided one. Several configurations of inverse tapers have been proposed in the literature, e.g., by exploring non-linear profiles [11], double tips [12], and tridents [13]. However, remarkable results in terms of coupling losses (<1 dB) and size (<hundreds of μm) have been achieved by using complex edge couplers, as with multiple SiN rods, knife edge shapes, or combining different materials [14], [15], [16]. Despite the highly promising performance results, the complicated and challenging fabrication process clashes with mass production. For the SiN platform, the

Manuscript received 18 July 2023; revised 15 August 2023; accepted 31 August 2023. Date of publication 4 September 2023; date of current version 13 September 2023. This work was supported in part by the New Satellites Generation Components (NSG) Project under Grant ARS_01_01_2015, in part by NoAcronym Programme (PoC #4 "RRPhCG"), and in part by "Giroscopio fotonico miniaturizzato ad alte prestazioni di nuova generazione" (GIFAP) under Project F96C1600000000S. *(Corresponding author: C. Ciminelli.)*

G. Brunetti, M. N. Armenise, and C. Ciminelli are with the Optoelectronics Laboratory, Politecnico di Bari, 70125 Bari, Italy (e-mail: giuseppe.brunetti@poliba.it; marionicola.armenise@poliba.it; caterina.ciminelli@poliba.it).

R. Heuvink and E. Schreuder are with LioniX BV, 7500 AL Enschede, The Netherlands (e-mail: r.w.h.heuvink@lionix-int.com; f.schreuder@lionix-int.com).

Color versions of one or more figures in this letter are available at https://doi.org/10.1109/LPT.2023.3311914.

Digital Object Identifier 10.1109/LPT.2023.3311914

lower refractive index contrast leads to a larger edge coupler length that enables the mode matching. Since the waveguide thickness is typically lower than 400 nm, the MFD matching of SMF with the waveguide requires the engineering of spot-size converters, to enlarge the mode field and reduce the coupling loss. By introducing SiOxN as the cladding layer of 300 nm x 300 nm SiN inverse tapers, a coupling loss of 0.85 dB was experimentally demonstrated in [24], while a coupling loss of 1.76 dB was obtained for a 700 nm x 200 nm waveguide embedded in a 700 × 700 SU-8 waveguide [25]. Also, the aspect ratio of the waveguide at the end of SSC plays a key role in guaranteeing low coupling loss. The geometry of the waveguide affects the mode size and shape, which in turn affects the coupling efficiency. In particular, the engineering of the waveguide aspect ratio tailors the mode profile to ensure high efficiency within a small footprint. Here, we demonstrate for the first time in literature the benefits of a high aspect ratio-based reverse SSC, that merges low propagation losses (of the order of dB/m at 1550 nm) with high coupling efficiency. An SSC with a minimum/maximum tip of 800 nm and 2.8 μm, respectively, and a total length of 600 μm has been designed by using the Beam Propagation Method (BPM). The design of the SSC has been carried out aiming at simultaneously matching all the requirements of compactness, low insertion loss, broad-band operation as well as ease of manufacture. About this point, all designed features result suitable for the fabrication at the current commercial Si-photonics fab, in contrast to concurrent reverse SSCs reported in the literature [26], which shows tip width less than 100 nm, that can be realized only by using electron-beam lithography or by using expensive ArF immersion lithography. The use of dedicated fabrication processes braked the use of reverse SSCs in commercial PICs. A coupling loss of less than 0.20 dB/facet has been experimentally proven over the whole C-band that fits well with the simulated results. According to our knowledge, the proposed SSC ensures the lowest coupling loss, combined with a large bandwidth, as reported in the literature, paving the way for using inverse SSC in high-volume PICs.

II. Proposed Spot Size Converter

The proposed SSC consists of an inverse taper L long whose narrow tip w_{MIN} wide is aligned to the SMF core. The SSC is able to convert large mode incident from the optical fiber, with an MFD on the order of 10 μm, to the compressed guided mode in the photonic waveguide w_{MAX} wide, as shown in Fig. 1(a). The bare waveguide is a SiO_2 fully embedded Si_3N_4 waveguide, with a thickness h of 100 nm and a width w (see Fig. 1(b)) whose fabrication is widely described in Section III. The interleaving of the thin core within SiO_2 cladding leads to a well laterally confined mode within the waveguide, also reducing the mode interaction with sidewalls and so the propagation losses (of the order of dB/m) [27]. For the design, the fundamental Transverse Electric (TE) mode has been taken into account, since it is mostly applied in optical communication applications. To properly engineer the proposed SSC, 2D Beam Propagation Method (BPM) simulations combined with the effective index method have been carried out by assuming SMF as a source with an MFD

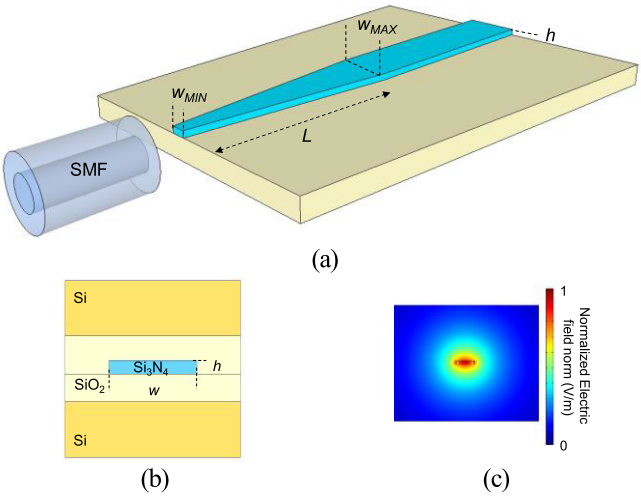

Fig. 1. (a) Si_3N_4 Spot Size Converter (SSC) with a length L and minimum/maximum tips with a width of w_{MIN}/w_{MAX}(SiO_2 - and Si - top cladding layers are not shown); (b) Si_3N_4 waveguide cross-section with a thickness h (= 100 nm) and width w; (c) TE distribution at the fiber tip (aspect ratio 8:1).

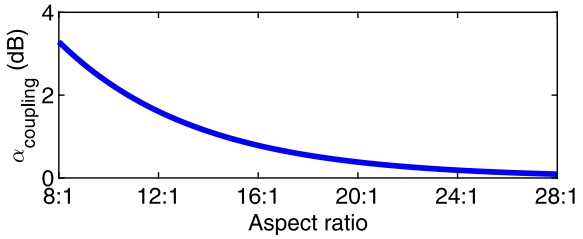

Fig. 2. $\alpha_{coupling}$ (dB) vs. Aspect ratio (w_{MAX}: h), by assuming L = 1000 μm and w_{MIN} = 0.8 μm, as the minimum width that ensures TE excitation.

of 10 μm. Firstly, to determine the optimal aspect ratio for the final waveguide, expressed as the ratio between width and thickness, a w_{MIN} of 0.8 μm has been considered. This is the minimum waveguide width that ensures the excitation of the TE mode.

Figure 2 shows the coupling losses $\alpha_{coupling}$ (dB) by varying the aspect ratio and considering a length of L = 1000 μm, which allows for nearly constant losses. The curve shows an exponential decreasing trend starting from 3.5 dB at the aspect ratio of 8:1 (w_{max} = 800 nm - h = 100 nm) up to 0.2 dB at the aspect ratio of 28:1 (w_{max} = 2.8 μm - h = 100 nm). As w_{max} increases, the confinement within the core and the MFD adiabatically increase (MFD = 3.6 μm with w_{max} = 2.8 μm), with a resulting decrease in the coupling losses. In Fig. 2, a maximum aspect ratio value of 28:1 has been considered both to avoid the excitation of higher order modes and to be compliant with the most promising waveguide reported in the current literature, which exhibits propagation loss on the order dB/m over the C-band [5]. To evaluate the impact of L and w_{MIN} on the performance, the contour plot of $\alpha_{coupling}$ is shown in Fig. 3(a), by considering h = 100 nm and w_{MAX} = 2.8 μm. Results show that the $\alpha_{coupling}$ losses increase with increasing w_{MIN}, while they adiabatically decrease as the length L increases due to the spread of the mode along the taper. The TE field distribution at the taper tip

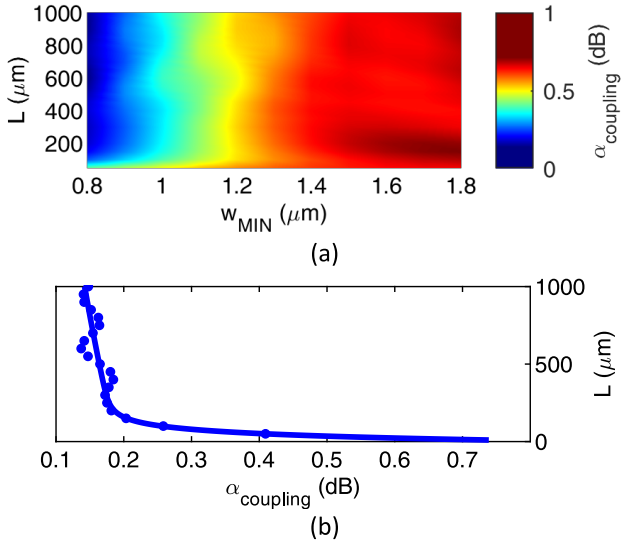

Fig. 3. (a) $\alpha_{coupling}$ (dB) contour plot vs. L and w_{MIN} with $w_{MAX} = 2.8$ μm; (b) $\alpha_{coupling}$ (dB) over L with $w_{MIN} = 0.8$ μm and $w_{MAX} = 2.8$ μm.

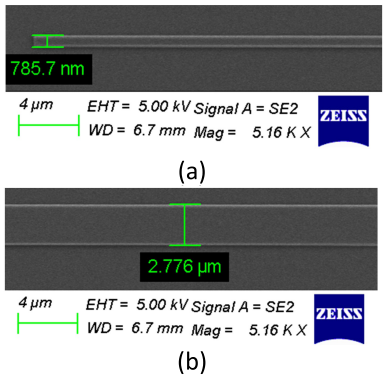

Fig. 4. SEM image of the SSC input (a) and output sections (b), with a resulting $w_{min} \approx 785$ nm and $w_{max} \approx 2.776$ μm.

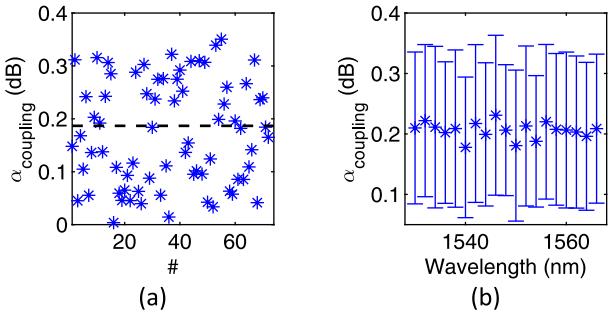

Fig. 5. (a) $\alpha_{coupling}$ (dB) at each facet of more than 70 devices (#) at 1550 nm; (b) $\alpha_{coupling}$ (dB) of the proposed SSC over the C-band. Error bars have been calculated by considering the standard deviation with respect to the mean value, labelled with stars.

with an aspect ratio 8:1 (Fig. 1(c)) leads to an overlap integral with the SMF mode of about 96.95 %. A length of 600 μm has been considered in the following with estimated losses of 0.18 dB. This length in the quasi-flat region of the trend (see Fig. 3(b)) ensures almost stable losses also by taking into account the fabrication tolerances.

The TM mode insertion loss analysis has been also carried out with the same approach as the TE one, with a simulated value of $\alpha_{coupling} = 0.6$ dB for $L = 1000$ μm.

III. SSC Fabrication

The fabrication of the SSC has been carried out at LioniX International BV. The device manufacturing started with a silicon substrate and a 15 μm thermally grown silicon dioxide layer. High-quality Si_3N_4 100 nm-thick was deposited via Low Pressure Chemical Vapour Deposition (LPCVD). Deep Ultraviolet (DUV) lithography allowed to define the waveguides and the SSC. Dry etching was used to etch through the Si_3N_4 film, thus defining the waveguide core widths. 1102 nm-thick SiO_2 layer was then deposited using TetraEthylOrthoSilicate (TEOS)-based LPCVD. A three-hour 1150 °C anneal was performed after the deposition, with a resulting shrinkage of the TEOS layer (thickness $\approx$ 1038 nm). The resulting protrusion of SiO_2 ($\approx$ 200 nm) above the waveguide cores was removed through Chemical Mechanical Polishing (CMP). After polishing, an additional silicon substrate with a 15 μm-thick SiO_2 layer was placed in contact with the starting wafer through wafer bonding at room temperature and pressure [28]. Since the quality of the chip facets is critical to improve the coupling losses, the facets were prepared by using mechanical dicing and then polishing to obtain a smooth sidewall with low surface roughness. Figs.4(a-b) show the SEM image of the SSC input- and output-section (at a distance of 1.004 mm to the input), respectively.

IV. Experimental Results

Due to the low coupling losses of SSCs, a cut-back method has been used to measure both the propagation losses and the coupling efficiency, by considering the loss of a device as the sum of the propagation loss in the straight section (proportional to the length) and twice the input section loss (assuming the input/output SSCs show the same losses). Fermat spirals with total lengths of 6.6 cm, properly engineered to avoid cross-coupling between waveguide coils and bending losses (minimum radii of 2 mm) [29], and multiple straight waveguides with lengths of about 13 mm have been used. For the experimental characterization of the devices under test, a frequency tunable laser (Keysight Technologies®81606A) with a linewidth $<$ 10 kHz and a frequency resolution of 1 nm within the range 1450-1650 nm have been used to excite the TE mode together with a fiber polarization controller. The input/output polarization maintaining FC/PC SMFs are placed close to the facets, with a spacing of the order of several microns. A refractive index-matching oil (Sigma Aldrich®AP100) has also been used to further reduce the scattering noise at facets caused by the undesired Fabry-Perot cavity between fibers and chip facets. Fig. 5(a) reports on the y-axis the coupling losses for each facet of the more than 70 fabricated devices at 1550 nm, reported on the x-axis. A mean value of $\alpha_{coupling}$ equal to 0.18 dB with a standard deviation σ of 0.12 dB has been experimentally measured.

A value of propagation losses of Si_3N_4-based waveguides and Fermat spirals of 13.16 $\pm$ 9.56 dB/m was measured, in accordance with other results reported in the literature [30].

Since the dispersion of Si_3N_4 varies by just 0.06% within the 1530 – 1570 nm range, a broadband operation over the C-band has been measured, as shown in Fig. 5(b). The mean value of $\alpha_{coupling}$ ranges from0.17 dB to 0.23 dB, demonstrating the feasibility of the proposed SSC in telecom PICs, with outstanding results improvement, in terms of coupling loss, with respect to the state-of-the-art [10], [11], [12], [13], [14], [15], [24], [25].

V. Conclusion

Optical interconnects in PICs are a critical issue to face to achieve efficient data transmissions. In particular, PICs often need to be coupled to optical fibers to become a functional part of optoelectronic systems. However, the mode mismatch between the fiber and the PIC leads to large coupling losses that could affect the performance of the overall system. Here, we report a quasi-lossless reverse SSC based on a Si_3N_4 waveguide, whose aspect ratio has been engineered to achieve the lowest coupling losses. An aspect ratio of 8:1 and 28:1 for the minimum and maximum tip, respectively, with a length of 600 μm guarantees coupling losses of 0.18 dB, as predicted by means of 2D-BPM simulations. Experimental results confirm the predicted losses ($= 0.18 \pm 0.12$ dB @ 1550 nm) with a broadband behavior over the whole C-band. To the best of our knowledge, the obtained outcomes represent the minimum coupling losses ever achieved in the C-band among the current state-of-the-art.

References

[1] R. Nagarajan et al., "Large-scale photonic integrated circuits," *IEEE J. Sel. Topics Quantum Electron.*, vol. 11, no. 1, pp. 50–62, Jan./Feb. 2005, doi: 10.1109/JSTQE.2004.841721.

[2] D. F. Welch et al., "The realization of large-scale photonic integrated circuits and the associated impact on fiber-optic communication systems," *J. Lightw. Technol.*, vol. 24, no. 12, pp. 4674–4683, Dec. 2006, doi: 10.1109/JLT.2006.885769.

[3] L. A. Coldren, S. W. Corzine, and M. L. Mašanović, *Diode Lasers and Photonic Integrated Circuits*. Hoboken, NJ, USA: Wiley, 2012, doi: 10.1002/9781118148167.

[4] H. Subbaraman et al., "Recent advances in silicon-based passive and active optical interconnects," *Opt. Exp.*, vol. 23, no. 3, p. 2487, Feb. 2015, doi: 10.1364/OE.23.002487.

[5] G. Son, S. Han, J. Park, K. Kwon, and K. Yu, "High-efficiency broadband light coupling between optical fibers and photonic integrated circuits," *Nanophotonics*, vol. 7, no. 12, pp. 1845–1864, Nov. 2018, doi: 10.1515/nanoph-2018-0075.

[6] M. J. R. Heck, J. F. Bauters, M. L. Davenport, D. T. Spencer, and J. E. Bowers, "Ultra-low loss waveguide platform and its integration with silicon photonics," *Laser Photon. Rev.*, vol. 8, no. 5, pp. 667–686, Sep. 2014, doi: 10.1002/lpor.201300183.

[7] A. Yariv and P. Yeh, *Optical Waves in Crystals: Propagation and Control of Laser Radiation*. Hoboken, NJ, USA: Wiley, 2003, p. 589. Accessed: May 19, 2023. [Online]. Available: https://www.wiley.com/en-us/Optical+Waves+in+Crystals%3A+Propagation+and+Control+of+Laser+Radiation-p-9780471430810

[8] M. Artiglia, G. Coppa, P. Di Vita, M. Potenza, and A. Sharma, "Mode field diameter measurements in single-mode optical fibers," *J. Lightw. Technol.*, vol. 7, no. 8, pp. 1139–1152, Aug. 1989, doi: 10.1109/50.32374.

[9] X. Mu, S. Wu, L. Cheng, and H. Y. Fu, "Edge couplers in silicon photonic integrated circuits: A review," *Appl. Sci.*, vol. 10, no. 4, p. 1538, Feb. 2020, doi: 10.3390/app10041538.

[10] M. Papes et al., "Fiber-chip edge coupler with large mode size for silicon photonic wire waveguides," *Opt. Exp.*, vol. 24, no. 5, pp. 5026–5038, Mar. 2016, doi: 10.1364/OE.24.005026.

[11] G. Ren, S. Chen, Y. Cheng, and Y. Zhai, "Study on inverse taper based mode transformer for low loss coupling between silicon wire waveguide and lensed fiber," *Opt. Commun.*, vol. 284, no. 19, pp. 4782–4788, Sep. 2011, doi: 10.1016/J.OPTCOM.2011.05.072.

[12] J. Wang et al., "Low-loss and misalignment-tolerant fiber-to-chip edge coupler based on double-tip inverse tapers," in *Proc. Opt. Fiber Commun. Conf. Exhib. (OFC)*, Mar. 2016, pp. 1–3, doi: 10.1364/OFC.2016.M2I.6.

[13] X. Tu et al., "Low polarization-dependent-loss silicon photonic trident edge coupler fabricated by 248 nm optical lithography," in *Proc. Asia Commun. Photon. Conf.*, Nov. 2015, Paper no. AS4B.3, doi: 10.1364/ACPC.2015.AS4B.3.

[14] M.-J. Picard et al., "CMOS-compatible spot-size converter for optical fiber to sub-μm silicon waveguide coupling with low-loss low-wavelength dependence and high tolerance to misalignment," *Proc. SPIE*, vol. 9752, pp. 132–138, Mar. 2016, doi: 10.1117/12.2208629.

[15] M. Pu, L. Liu, H. Ou, K. Yvind, and J. M. Hvam, "Ultra-low-loss inverted taper coupler for silicon-on-insulator ridge waveguide," *Opt. Commun.*, vol. 283, no. 19, pp. 3678–3682, Oct. 2010, doi: 10.1016/J.OPTCOM.2010.05.034.

[16] R. Takei et al., "Silicon knife-edge taper waveguide for ultralow-loss spot-size converter fabricated by photolithography," *Appl. Phys. Lett.*, vol. 102, no. 10, Mar. 2013, Art. no. 101108, doi: 10.1063/1.4795308.

[17] W. Zhang et al., "Buried 3D spot-size converters for silicon photonics," *Optica*, vol. 8, no. 8, pp. 1102–1108, Aug. 2021, doi: 10.1364/OPTICA.431064.

[18] Z. Xiao, F. Luan, J. Zhang, P. Shum, and T.-Y. Liow, "Design for broadband high-efficiency grating couplers," *Opt. Lett.*, vol. 37, no. 4, pp. 530–532, Feb. 2012, doi: 10.1364/OL.37.000530.

[19] L. He et al., "A high-efficiency nonuniform grating coupler realized with 248-nm optical lithography," *IEEE Photon. Technol. Lett.*, vol. 25, no. 14, pp. 1358–1361, Jul. 15, 2013, doi: 10.1109/LPT.2013.2265911.

[20] R. Halir et al., "Continuously apodized fiber-to-chip surface grating coupler with refractive index engineered subwavelength structure," *Opt. Lett.*, vol. 35, no. 19, pp. 3243–3245, Oct. 2010, doi: 10.1364/OL.35.003243.

[21] D. Vermeulen et al., "High-efficiency fiber-to-chip grating couplers realized using an advanced CMOS-compatible silicon-on-insulator platform," *Opt. Exp.*, vol. 18, no. 17, pp. 18278–18283, Aug. 2010, doi: 10.1364/OE.18.018278.

[22] Y. Xue, H. Chen, Y. Bao, J. Dong, and X. Zhang, "Two-dimensional silicon photonic grating coupler with low polarization-dependent loss and high tolerance," *Opt. Exp.*, vol. 27, no. 16, p. 22268, Aug. 2019, doi: 10.1364/OE.27.022268.

[23] M. Streshinsky et al., "A compact bi-wavelength polarization splitting grating coupler fabricated in a 220 nm SOI platform," *Opt. Exp.*, vol. 21, no. 25, p. 31019, Dec. 2013, doi: 10.1364/OE.21.031019.

[24] Z. Li et al., "Ultra-low loss SiN edge coupler interfacing with a single-mode fiber," *Opt. Lett.*, vol. 47, no. 18, pp. 4786–4789, Sep. 2022, doi: 10.1364/OL.469708.

[25] P. J. Cegielski et al., "Silicon nitride waveguides and spot size converters with $<$ 1.76 dB loss over broad wavelength range from 1010 nm to 1110 nm for OCT applications," in *Proc. Passive Photonic Integr. Struct. New Platforms, Eur. Conf. Integr. Opt. (ECIO)*, Nov. 2020, pp. 1–3.

[26] J. Zhao, Z. Wang, N. Ye, F. Pang, and Y. Song, "The low-loss spot size converter for alignment with cleaved single mode fiber," *Appl. Sci.*, vol. 13, no. 14, p. 8157, Jul. 2023, doi: 10.3390/app13148157.

[27] J. F. Bauters et al., "Ultra-low-loss high-aspect-ratio Si_3N_4 waveguides," *Opt. Exp.*, vol. 19, no. 4, pp. 3163–3174, Feb. 2011, doi: 10.1364/OE.19.003163.

[28] J. Bauters et al., "Planar waveguides with less than 0.1 dB/m propagation loss fabricated with wafer bonding," *Opt. Exp.*, vol. 19, no. 24, pp. 24090–24101, Nov. 2011, doi: 10.1364/OE.19.024090.

[29] G. Brunetti, F. Dell' Olio, D. Conteduca, M. N. Armenise, and C. Ciminelli, "Comprehensive mathematical modelling of ultra-high Q grating-assisted ring resonators," *J. Opt.*, vol. 22, no. 3, Feb. 2020, Art. no. 035802, doi: 10.1088/2040-8986/AB71EB.

[30] M. Belt et al., "Sidewall gratings in ultra-low-loss Si_3N_4 planar waveguides," *Opt. Exp.*, vol. 21, no. 1, pp. 1181–1188, Jan. 2013, doi: 10.1364/OE.21.001181.

Open Access funding provided by 'Politecnico di Bari' within the CRUI CARE Agreement